Cancer Science
Japanese Cancer Association JCA
Open Access

Low-dose paclitaxel improves the therapeutic efficacy of recombinant adenovirus encoding CCL21 chemokine against murine cancer

Ping Chen,[1,2,3,5] Shan Luo,[1,3,5] Yan-Jun Wen,[1] Yu-Hua Li,[1,2] Jiong Li,[1] Yong-Sheng Wang,[1] Li-Cheng Du,[1,4] Ping Zhang,[1] Jiao Tang,[1] Da-Bing Yang,[1] Huo-Zhen Hu,[1] Xia Zhao[1] and Yu-Quan Wei[1]

[1]State Key Laboratory of Biotherapy and Cancer Center, West China Hospital, West China Medical School, Sichuan University, Chengdu; [2]National Institutes for Food and Drug Control, Beijing; [3]Chengdu Institute of Biological Products Co., Ltd, Chengdu; [4]Provincial Hospital affiliated to Shandong University, Shandong, China

Key words

Angiogenesis, CCL21, cytotoxic T lymphocytes, immunotherapy, paclitaxel

Correspondence

Yu-Quan Wei, State Key Laboratory of Biotherapy and Cancer Center, West China Hospital, West China Medical School, Sichuan University, 1# Keyuan Road 4, Gaopeng Street, High Technological Development Zone, Chengdu, Sichuan 610041, China.
Tel: 86-28-85250731; Fax: +86-28-85250731;
E-mail: yuquawei@vip.sina.com

[5]These authors contributed equally to this work.

Funding information

The National Key Basic Research Program (973 Program) of China (2010CB529900). (2010CB529906). Hi-tech Research and Development Program (863 Program) of China (2007AA021106). (2006AA02Z488).

Received May 9, 2014; Revised September 2, 2014; Accepted September 3, 2014

Cancer Sci **105** (2014) 1393–1401

doi: 10.1111/cas.12537

Secondary lymphoid tissue chemokine (SLC/CCL21), one of the CC chemokines, exerts potent antitumor immunity by co-localizing T cells and dendritic cells at the tumor site and is currently tested against human solid tumors. Here, we investigated whether the combination of recombinant adenovirus encoding murine CCL21 (Ad-mCCL21) with low-dose paclitaxel would improve therapeutic efficacy against murine cancer. Immunocompetent mice bearing B16-F10 melanoma or 4T1 breast carcinoma were treated with either Ad-mCCL21, paclitaxel, or both agents together. Our results showed that Ad-mCCL21 + low-dose paclitaxel more effectively reduced the growth of tumors as compared with either treatment alone and significantly prolonged survival time of the tumor-bearing animals. These antitumor effects of the combined therapy were linked to altered cytokine network at the tumor site, enhanced apoptosis of tumor cells, and decreased formation of new vessels in tumors. Importantly, the combined therapy elicited a strong therapeutic antitumor immunity, which could be partly abrogated by the depletion of $CD4^+$ or $CD8^+$ T lymphocytes. Collectively, these preclinical evaluations may provide a combined strategy for antitumor immunity and should be considered for testing in clinical trials.

Induction of an effective antitumor immune response is a complex process requiring coordinate interaction of different subsets of effector cells, including antigen-presenting cells, lymphocytes, and natural killer (NK) cells.[1–3] However, tumor cells often express limited MHC antigens and lack co-stimulatory molecules; they are ineffective antigen-presenting cells.[4] In addition, many tumor cells produce immunosuppressive cytokines that promote escape from immune surveillance.[5] Thus, enlisting the host response to recognize poorly immunogenic tumors, and altering the immunologic intratumoral microenvironment may be beneficial for the treatment of cancer.

Chemokines are a family of structurally related proteins that activate inflammatory responses, regulate leukocyte trafficking, and participate in many other pleiotropic functions, including regulation of tumor growth.[6,7] The CC chemokine CCL21, also known as secondary lymphoid chemokine or C6kine, is mainly and constitutively expressed in high endothelial venules and in T-cell zones of spleen, lymph nodes, and Peyer's patches.[8,9] Previous studies have established that CCL21 exerts potent chemotactic activity on T cells, B cells, and dendritic cells (DCs).[10–12] The capacity to co-localize DCs and lymphocytes makes CCL21 a good therapeutic candidate against cancer. Accordingly, intratumoral treatment with recombinant CCL21 or CCL21-gene-modified DCs would lead to immune-mediated tumor growth inhibition.[13–17] However, for the multifaceted nature of the tumor microenvironment, the antitumoral response of CCL21 is not sufficiently robust, which suggests that further treatment may require supplemental drugs.

Paclitaxel, a prototypic taxane compound, which exerts its cytotoxic effect by inducing G_2/M phase arrest and apoptosis in tumor cells, is one of the most active agents used for the clinical treatment of cancer.[18,19] However, dose-dependent toxicity and drug resistance greatly limit the clinical application of paclitaxel. One promising strategy to reduce the toxicity of chemotherapy is frequent protracted use of low-dose conventional cytotoxic drugs on a metronomic schedule.[20,21] Several recent studies from other groups have indicated that low-dose paclitaxel might alter the intratumoral immunologic microen

vironment, including cytokine network and immunosuppressive activity of tumor cells, which suggests that low-dose paclitaxel may improve the outcome of immunotherapy with less toxicity.[22,23] Thus, we wondered whether it would improve the therapeutic and primary immunologic effects of the antitumor by combining low-dose paclitaxel with CCL21. The present article showed that this combined therapy would induce superior antitumor activity.

Materials and Methods

Cell lines and animals. Human cervical carcinoma cell line Hela, human embryo kidney cell line 293, murine melanoma cell line B16-F10, and murine breast carcinoma cell line 4T1 were obtained from the ATCC (Manassas, VA, USA). B16-F10 cells were cultured in DMEM, and 4T1 cells were cultured in RPMI-1640, each supplemented with 10% FBS. Female C57BL/6 and BALB/c mice, 6–8 weeks old, were purchased from the Laboratory Animal Center of Sichuan University (Sichuan, China). All studies involving mice were carried out in conformity with institutional guidelines concerning animal use and care.

Construction of recombinant adenoviral vector encoding murine CCL21. The nucleotide sequence encoding the mature region of murine CCL21 cDNA was PCR amplified from pORF5-mExodus2 (InvivoGen, San Diego, CA, USA) and cloned into pENTR11 vector (Invitrogen, Carlsbad, CA, USA). The resulting plasmid was recombined with destination vector according to the manufacturer's instructions. The viral particles (Ad-mCCL21) were produced and amplified in 293 cells, purified by two-step CsCl gradient ultracentrifugation. The virus titer was quantified using a standard TCID50 assay.[24] The recombinant adenovirus containing the *LacZ* gene (Ad-LacZ) served as a control.

***In vitro* infection with recombinant adenovirus.** Hela cells were infected at an MOI of 100 (10^8 p.f.u. per 10^6 cells in 1 mL complete media) with Ad-mCCL21, Ad-LacZ, or no transduction. Forty-eight hours after infection, cells were harvested and analyzed by Western blotting using a rabbit anti-murine mCCL21 monoclonal IgG antibody (Peprotech EC, London, UK). To detect the supernatant mCCL21 concentrations, 4T1 cells were infected at MOI ranging from 0.1 to 100 with Ad-mCCL21 or Ad-LacZ. Supernatants were harvested 48 h after infection and the mCCL21 concentrations were analyzed with an ELISA kit (Boster, Wuhan, China).

Functional assay of virally generated mCCL21. Biological activity of virally generated mCCL21 was evaluated by chemotaxis as previously described.[25] Briefly, 50 μL 4T1 cell culture supernatant was added to the bottom wells of a 96-well Boyden microchamber's chemotaxis plate (Neuroprobe, Gaithersburg, MD, USA). Then 50 μL lymphocyte cells (2×10^6 cells/mL migration medium) were added to the upper compartment of the migration chamber (5-μm pore size, polycarbonate filters, polyvinylpyrrolidone-free polycarbonate membranes). For the blocking experiments, cell culture supernatant was added with 30 μg/mL rabbit anti-mCCL21 antibody (Peprotech EC) or control rabbit IgG (Sigma-Aldrich, St Louis, MO, USA). The chemotaxis plate was incubated at 37°C for 4 h and transferred to 4°C for 10 min. Then the membrane was fixed in 70% methanol and stained with Wright's stain for 5 min. The number of cells that migrated to the lower surface was counted on six randomly selected high power fields. Commercially murine CCL21 (Peprotech EC) with biological activity served as the standard control.

***In vivo* production of mCCL21.** To assess the duration and amount of mCCL21 expression, mice bearing 4T1 breast carcinoma were intratumorally injected with 5×10^8 p.f.u. Ad-mCCL21 or Ad-LacZ, or no virus. On days 0, 2, 4, 6, and 8, mice were euthanized with carbon dioxide, and the tumor tissue were harvested, cut into small pieces, homogenized, and centrifuged at 12 000*g* for 30 min. The concentrations of mCCL21 in the supernatants were determined by ELISA as described previously.[26] Tumor-derived mCCL21 concentrations were corrected for total protein by Lowry protein assay (Thermo Fisher Scienfic, Rockford, IL, USA), and the results were expressed as pg/mg total protein.

Tumor growth inhibition study. B16-F10 melanoma and 4T1 breast carcinoma models were established in immunocompetent C57BL/6 and BALB/c female mice at 6–8 weeks of age, respectively, as previously described.[26] Mice were randomly divided into five groups when the size of tumors reached approximately 30 mm^3 (about 6 days after tumor cell inoculation), and received the corresponding treatment: normal saline (NS, 100 μL); paclitaxel (Pac, 40 μg/mouse, 100 μL); Ad-mCCL21 (5×10^8 p.f.u., 100 μL); Ad-LacZ+Pac (Ad-LacZ, 5×10^8 p.f.u., 100 μL; paclitaxel, 40 μg/mouse, 100 μL); or Ad-mCCL21+Pac (Ad-mCCL21, 5×10^8 p.f.u., 100 μL; paclitaxel, 40 μg/mouse, 100 μL). Normal saline and the viral particles were injected at several points into the tumors on days 6, 11, 16, and 21 after tumor cell inoculation. Paclitaxel was delivered intrapleurally on the same schedule as above. The experiment for the observation of tumor growth and survival advantage included 10 mice per group. Tumor dimensions were measured with calipers every 3 days, and tumor volumes were calculated according to the formula $V = \pi/6 \times \text{length (mm)} \times \text{width (mm)} \times \text{width (mm)}$, where length is the longest dimension and width is the shortest dimension. For the histological analysis, the mice were killed by cervical dislocation on day 4 after the completion of treatment as described above. Autopsy was carried out to determine the number and diameter of the metastatic nodules. Tumors and tissues were excised and fixed in 10% neutral buffered formalin solution or frozen at −80°C.[25]

Histological analysis. Tissues from each group were embedded in paraffin. Sections 3–5-μm thick were stained with H&E. Expression of CCL21 was determined by immunostaining with an anti-mCCL21 mAb (Peprotech EC). To determine whether the antitumor effects of the combined therapy were involved in the inhibition of angiogenesis, neovascularization in the tumor tissues was determined by immunohistological analysis with an anti-CD31 antibody (Thermo Fisher Scienfic, Rockford, IL, USA). Vessel density was determined by counting the number of microvessels per high-power field in the sections, as described.[4]

Immunofluorescence staining was used to determine the infiltration of immune cells in the tumor tissue. Tumors were snap-frozen and 8-μm sections were prepared in Tissue Tek (Sakura Finetek) for immunofluorescence analysis. Anti-CD4 (FITC conjugate; eBioscience) and anti-CD8 (Cy5PE conjugate; eBioscience) mAbs were used to determine the T lymphocytes, whereas anti-CD11c (Cy5PE conjugate; BD Bioscience) mAbs were used to detect dendritic cells. Fluorescence was visualized, and images were captured with fluorescence microscopy (Leica).

Quantitative assessment of apoptosis. Paraffin sections were prepared as described above. The presence of apoptotic cells within the tumor sections was determined using a TUNEL Kit (DeadEnd Fluorometric TUNEL System; Promega) following the manufacturer's protocol. In tissue sections, apop-

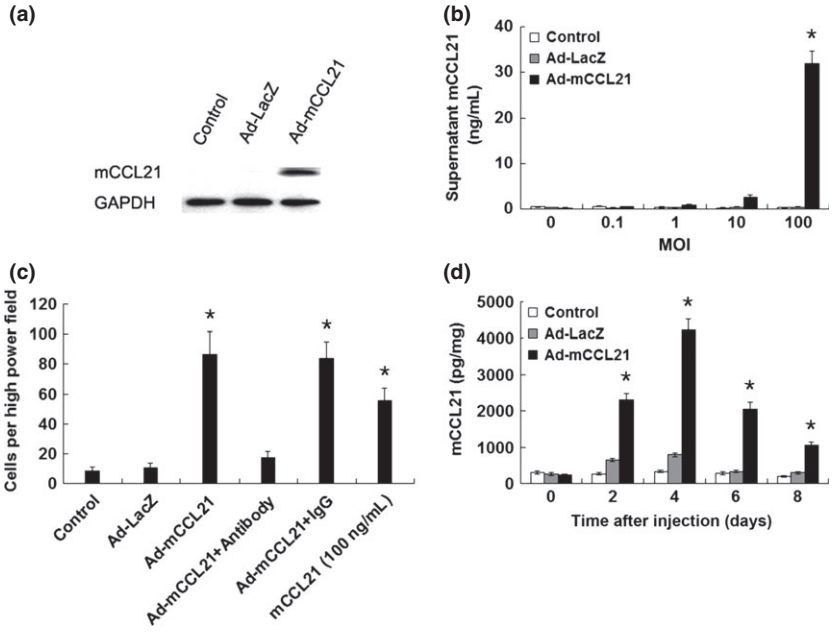

Fig. 1. *In vitro* and *in vivo* expression and biological activity of murine CCL21. (a) Western blot analysis of murine CCL21 expression after infection of Hela cells. (b) 4T1 cells were infected with Ad-mCCL21 or Ad-LacZ at varying MOIs, yielding dose-dependent supernatant mCCL21 concentrations up to 31.9 ± 2.7 ng/mL after Ad-mCCL21 infection. (c) Chemotactic assay of conditioned medium from infected 4T1 cells. Supernatants from Ad-mCCL21 infected 4T1 cells (MOI = 100) clearly attracted lymphocytes, with a superior capacity for chemotaxis compared with purchased mCCL21 *in vitro*. (d) Tumor mCCL21 levels 0–8 days after a single intratumoral injection of Ad-mCCL21. Levels were 4220.1 ± 303.5 pg/mg at 4 days and remained significantly higher than controls at day 8. Bars, ±SD. **P* < 0.01, significantly different from the controls.

totic cells were counted under a microscope (×200) in five randomly selected fields. The apoptotic index was calculated as a ratio of the total tumor cell number in each high-powered field.

Cytokine-specific ELISA. Mice bearing 4T1 breast carcinoma were treated with various therapies stated above, and on day 4 after the completion of treatment, cytokine protein concentrations from tumor nodules were determined by ELISA as described previously.[14] Tumor tissues were harvested, cut into small pieces, homogenized, and centrifuged at 12 000*g* for 30 min. Cytokines (granulocyte–macrophage colony-stimulating factor [GM-CSF], γ-interferon [IFN-γ], monokine induced by interferon-gamma [MIG], interferon-gamma-induced protein 10 [IP-10], interleukin-12 [IL-12], transforming growth factor-β [TGF-β], IL-10, and vascular endothelial growth factor [VEGF]) were determined by ELISA in homogenized tumors directly. Tumor-derived cytokine concentrations were corrected for total protein by Lowry protein assay (Thermo), and the results were expressed as pg/mg total protein.

γ-Interferon enzyme-linked immunospot assay. To evaluate the immune specificity of the treatments, IFN-γ enzyme-linked immunospot (ELISPOT) assay was carried out to determine the frequency of T lymphocytes producing IFN-γ in response to specific tumors. On day 4 after cessation of treatment, splenic T lymphocytes from mice bearing 4T1 breast carcinoma were purified with Nylon Fiber Column T (L-Type; Wako). T lymphocytes were co-incubated with either 4T1 cells or non-specific syngeneic CT26 cells at a lymphocyte effector-to-stimulator ratio of 5:1 for 24 h. Spots were quantified with the use of computer-assisted video image analysis as described previously.[27]

***In vitro* cytotoxicity assay.** The ^{51}Cr release assay was carried out to evaluate the adaptive cellular immune response as described previously.[26] Briefly, 4T1 breast carcinoma-bearing animals received therapy as described above. On day 4 after the complement of the treatment, splenic T lymphocytes were isolated from single-cell suspensions with Nylon Fiber Column T (L-Type; Wako) as CTL effector cells. The 4T1 breast carcinoma cells were used as target cells by incubation at 37°C with ^{51}Cr for 2 h. Effector and target cells were seeded into the 96-well microtiter plate at different effector/target (E/T) ratios, and incubated for 4 h at 37°C. The supernatant was harvested, and the CTL activity was calculated by the following formula: %cytotoxicity = [(experimental release − spontaneous release) /(maximum release − spontaneous release)] × 100.

***In vivo* depletion of immune cell subsets.** Immune cell subsets were depleted as described previously.[28] Briefly, mice bearing 4T1 breast carcinoma received i.p. injections of 500 μg of either the anti-CD4 (clone GK1.5, rat IgG), anti-CD8 (clone 2.43, rat IgG), anti-NK (clone PK136) mAb, or isotype controls, 1 day before the combined treatment and then twice per week for 3 weeks. These hybridomas were obtained from ATCC. Tumors were excised and weighed on day 7 after the completion of treatment.

Statistical analysis. Data were assayed by ANOVA and an unpaired Student's *t*-test. Kaplan–Meier curves were established for each group of animals, and survival curves were compared by the log–rank test. Differences between means or ranks, as appropriate, were considered significant when yielding a $P < 0.05$.

Results

***In vitro* and *in vivo* expression and biological activity of murine CCL21.** We first cloned the murine *CCL21* gene into an adenoviral shuttle plasmid and generated recombinant Ad-mCCL21. The expression of mCCL21-infected Hela cells was confirmed by Western blot analysis (Fig. 1a). Murine 4T1 breast carcinoma cells were infected with Ad-mCCL21 or Ad-LacZ. A dose-dependent elevation of supernatant mCCL21 concentrations was observed in Ad-mCCL21-infected cells, up to 31.9 ± 2.7 ng/mL at a MOI of 100 (Fig. 1b). The *in vitro* biological activity of mCCL21 was tested using a chemotaxis assay. Commercially available recombinant murine CCL21 from Peprotech was used as the standard control. The results suggested that conditioned medium from Ad-mCCL21-infected 4T1 cells has a superior capacity of chemotaxis compared with purchased mCCL21 *in vitro* (Fig. 1c).

In vivo expression of mCCL21 was assessed in the 4T1 tumor tissues after intratumoral delivery of Ad-mCCL21, Ad-LacZ, or

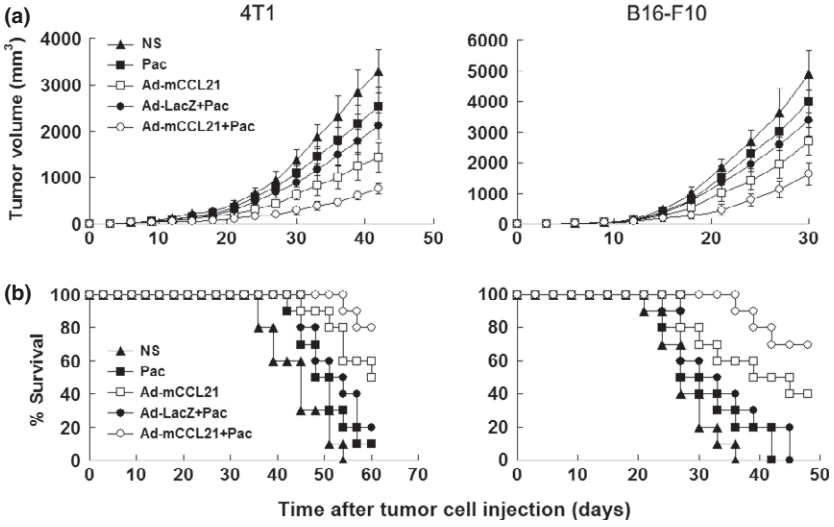

Fig. 2. Tumor suppression and survival advantage in mice. Immunocompetent C57BL/6 and BALB/c mice bearing B16-F10 melanoma and 4T1 breast carcinoma were treated with normal saline (NS), paclitaxel (Pac), Ad-mCCL21, Ad-LacZ+Pac, or Ad-mCCL21+Pac. (a) Suppression of s.c. tumor growth in mice. Ad-mCCL21+Pac treatment resulting in significant tumor growth inhibition *versus* NS controls ($P < 0.01$), Pac ($P < 0.01$), Ad-mCCL21 ($P < 0.05$), or Ad-LacZ+Pac ($P < 0.01$) from day 20 after initiation of treatment. Points, average tumor volume; bars, ±SD. (b) A significant increase was observed in the survival rates of Ad-mCCL21+Pac treatment mice compared with the other groups ($P < 0.01$, by log–rank test).

sterile NS. Peak expression of mCCL21 was observed 4 days after injection, at which time the mCCL21 concentrations were 4220.1 ± 303.5 pg/mg. On day 8, intratumoral levels of mCCL21 remained significantly elevated (1050.7 ± 95.3 pg /mg *vs* 291.4 ± 29.0 pg/mg in Ad-LacZ-treated animals; $P < 0.01$) (Fig. 1d).

Tumor growth inhibition. We evaluated the antitumor activity of the combination therapy in the immunocompetent C57BL/6 and BALB/c mice bearing B16-F10 melanoma and 4T1 breast carcinoma, respectively. The results showed that Ad-mCCL21 or low-dose paclitaxel alone inhibited tumor growth to a certain extent. However, combined treatment with Ad-mCCL21 and low-dose paclitaxel had a superior antitumor effect, resulting in more than 66% and 78% inhibition in tumor volume compared with the NS group in B16-F10 and 4T1 ($P < 0.01$, 4 days after the completion of treatment; Fig. 2a). In the two tumor models, control animals that received NS treatment survived 44.1 and 27.7 days on average, respectively. In contrast, the combined treatment resulted in a significant twofold increase in life span ($P < 0.01$, log–rank test; Fig. 2b). Additionally, the appearance of lung metastases in the 4T1 model was significantly delayed by treatment with Ad-mCCL21 or Ad-mCCL21+Pac in comparison with NS control (data not shown).

Inhibition of tumor angiogenesis. Angiogenesis within tumor tissues was estimated in sections by staining with an antibody reactive to CD31. The most highly vascularized area of each tumor was identified on low power and five high-powered fields were counted in this area of greatest vessel density. The combination of Ad-mCCL21 and paclitaxel apparently reduced the number of vessels compared with the control groups, including NS, paclitaxel, or Ad-null+Pac. The reduced vessel density could also be observed in the Ad-mCCL21-treated group. No statistically significant difference was found between paclitaxel and Ad-null+Pac groups (Fig. 3a).

Therapeutic effect on apoptosis. To explore the role of combined therapy on apoptosis of tumor cells, tumors resected 4 days after the completion of treatment were subjected to

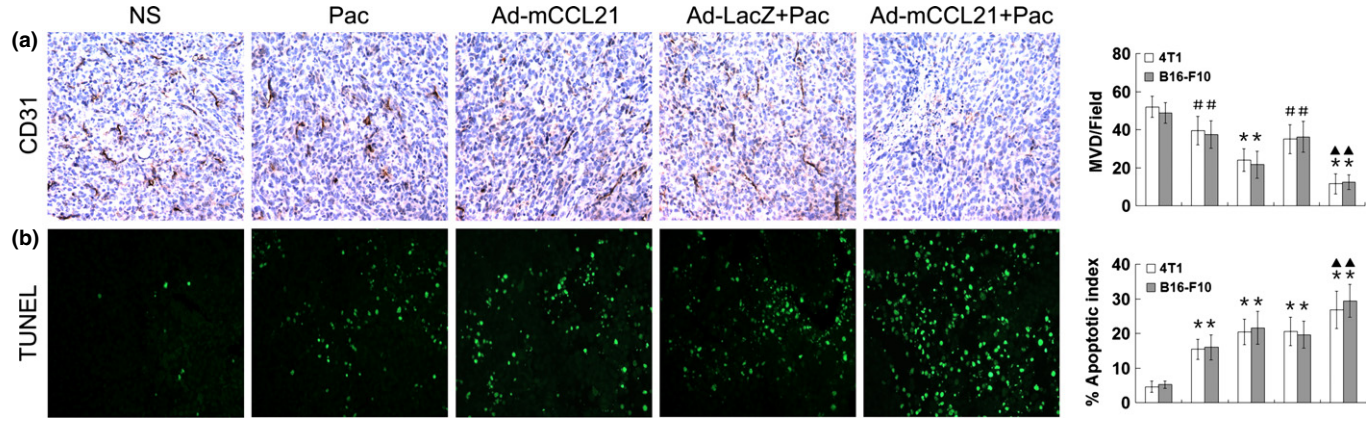

Fig. 3. Histochemical analysis of tumors. (a) Tumor angiogenesis was determined by staining paraffin-embedded sections with anti-CD31 antibody. The number of vessels per ×200 field was counted. Occasionally, isolated microvessels could be found in Ad-mCCL21 + low-dose paclitaxel (Ad-mCCL21+Pac)-treated tumors. Ad-mCCL21, Pac, or Ad-LacZ treatment also has an angiostatic effect. At the same magnification, the well-formed capillaries surrounding nests of tumor cells could be found in the normal saline (NS) control group. (b) Apoptotic tumor cells within tumor tissues were elevated by TUNEL assays. The apoptotic index was calculated as a ratio of the apoptotic cell number to the total cell number in each field. Sequential analysis showed that Ad-mCCL21+Pac treatment resulted in significant increment of apoptotic index *versus* NS control. Pac, Ad-mCCL21, and Ad-LacZ+Pac also efficiently induced the apoptosis of tumor cells. The columns in all graphs correspond to the labeled columns in the picture. Bars, ±SD. *$P < 0.01$ relative to NS control. ▲$P < 0.01$ relative to Pac, Ad-mCCL21, or Ad-LacZ+Pac group. MVD, microvessel density, #$P < 0.05$ relative to NS control.

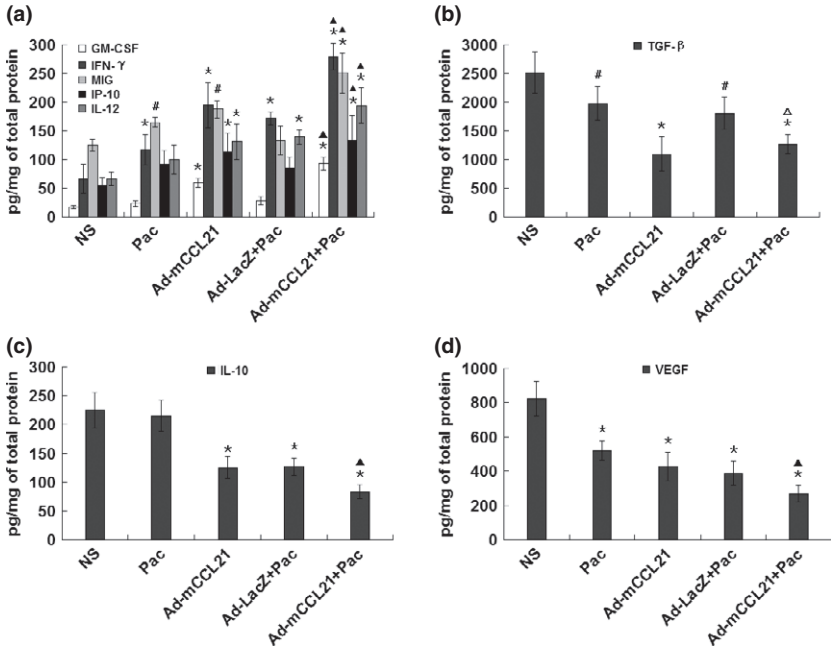

Fig. 4. Analysis of cytokines in the tumor site. Mice bearing 4T1 breast carcinoma were treated with normal saline (NS), paclitaxel (Pac), Ad-mCCL21, Ad-LacZ+Pac, or Ad-mCCL21+Pac. On day 4 after the completion of treatment, tumor tissues were harvested, cut into small pieces, homogenized, and centrifuged at 12 000*g* for 30 min. Tumors were evaluated for the presence of granulocyte–macrophage colony-stimulating factor (GM-CSF), γ-interferon (IFN-γ), monokine induced by interferon-gamma (MIG), interferon-gamma-induced protein 10 (IP-10), interleukin-12 (IL-12), transforming growth factor-β (TGF-β), IL-10, and vascular endothelial growth factor (VEGF) by ELISA. Cytokine concentrations were corrected for total protein by Lowry protein assay. Results are expressed as pg/mg total protein. Compared with tumor tissues from the NS control group, mice treated with Ad-mCCL21+Pac had significant increase in GM-CSF, IFN-γ, MIG, IP-10, and IL-12 (a) but a decrease in TGF-β (b), IL-10 (c), and VEGF (d). Bars, ±SD. $*P < 0.01$ relative to NS control. $\#P < 0.05$ relative to NS control. $\blacktriangle P < 0.01$ relative to Pac, Ad-mCCL21, or Ad-LacZ+Pac group. $\triangle P < 0.01$ relative to Pac or Ad-LacZ+Pac group.

TUNEL assays. Paclitaxel, Ad-mCCL21, or Ad-null+Pac treatment affected the apoptotic rate of tumor cells, whereas an apparent increase in the number of apoptotic cells was observed within the tumors of Ad-mCCL21+Pac treated group (Fig. 3b). The apoptotic index (AI) was defined as follows: AI (%) = 100×apoptotic cells/total tumor cells.

Contribution of cytokines in tumor growth delay. To determine the relative contribution of cytokines to the tumor growth delay observed in the combined treated group, we measured the cytokine production from tumor sites following therapy. The tumor tissues were evaluated in the presence of GM-CSF, IFN-γ, MIG, IP-10, IL-12, TGF-β, IL-10, and VEGF by ELISA. Compared with the controls, animals receiving Ad-mCCL21 had a modest but significant increase in type 1 cytokine (IFN-γ and IL-12) and antiangiogenic chemokines (MIG and IP-10) and a decrease in the immunosuppressive mediators (TGF-β) at the tumor sites. However, as was evident for tumor reduction, the combined treatment most effectively altered the cytokine network at the tumor microenvironment. Compared with the NS group, combined treatment significantly reduced the expression of IL-10 (2.7-fold; $P < 0.01$), TGF-β (2.0-fold; $P < 0.01$), and VEGF (3.1-fold; $P < 0.01$). This was coupled with an increase in GM-CSF (5.4-fold; $P < 0.01$), IFN-γ (4.2-fold; $P < 0.01$), MIG (2.0-fold; $P < 0.01$), IP-10 (2.4-fold; $P < 0.01$), and IL-12 (2.9-fold; $P < 0.01$) within the tumor sites (Fig. 4).

Expression of mCCL21 within tumor results in recruitment immune cell subsets. Immunohistochemical staining was done to detect intratumoral expression of mCCL21. The results indicated that mCCL21 can be effectively expressed and secreted from tumor cells in the tumor tissues. No significantly different distribution of CCL21 was found in the tissues of Ad-mCCL21- and Ad-mCCL21+Pac-treated groups in the present study. In order to test whether the combined therapy elevated the infiltration of immune cells, tumors resected 4 days after the completion of treatment were subjected to immunofluorescence assay. The infiltration of lymphocytes and dendritic cells was apparently found in the tumor tissues of both Ad-mCCL21 alone and Ad-mCCL21 in conjunction with paclitaxel groups. Paclitaxel or Ad-null+Pac treatment also affected the infiltration of immune cells (Fig. 5).

Combined therapy induces specific T-cell responses. To determine whether the therapy induces specific T-cell responses, IFN-γ ELISPOT assays were carried out. The combination of mCCL21 and paclitaxel had significantly greater frequency of specific T cells releasing IFN-γ when restimulated with 4T1 cells ($P < 0.01$ relative to NS control). AdmCCL21, paclitaxel, or Ad-LacZ+Pac treatment also induced significant specific T-cell responses to 4T1 cells as compared to the NS group ($P < 0.01$). The minimal responses to control CT26 cells could be observed in the AdmCCL21, paclitaxel, Ad-LacZ+Pac, and Ad-mCCL21+Pac treatment group (Fig. 6a).

Effect of combination therapy on cytotoxic T-lymphocyte activities. Determination of CTL activity provided evidence for the involvement of an immunological mechanism in the antitumor effects of the treatments. As shown in Figure 6(b), splenic T lymphocytes isolated from mice (4T1 model) treated with Ad-mCCL21 or Ad-mCCL21+Pac were able to lyse specific target cells (4T1 cells) in an E/T-dependent manner with statistical significance at E/T ratios ≥10:1. These results suggested that Ad-mCCL21 alone or Ad-mCCL21 plus paclitaxel could efficiently induce tumor-specific CTL response *in vivo*.

Function of T-cell subsets in antitumor activity. To explore the roles of immune cell subsets in this antitumor activity elicited by the combined therapy, we depleted $CD4^+$ or $CD8^+$ T lymphocytes or NK cells through injection of the corresponding antibodies. As shown in Figure 6(c), depletion of $CD4^+$ or $CD8^+$ T lymphocytes could significantly decrease the antitumor activity of the combined therapy, whereas the depletion of NK cells slightly abrogate the antitumor activity. These findings indicate both $CD4^+$ and $CD8^+$ T lymphocytes were involved in this therapy-induced antitumor activity.

Observation of potential toxicity. To evaluate the possible adverse effects of the combined treatment, Ad-mCCL21+Pac-treated animals without tumor burden were particularly investigated for potential toxicity for more than 4 months. No adverse consequences were indicated in gross measures, such

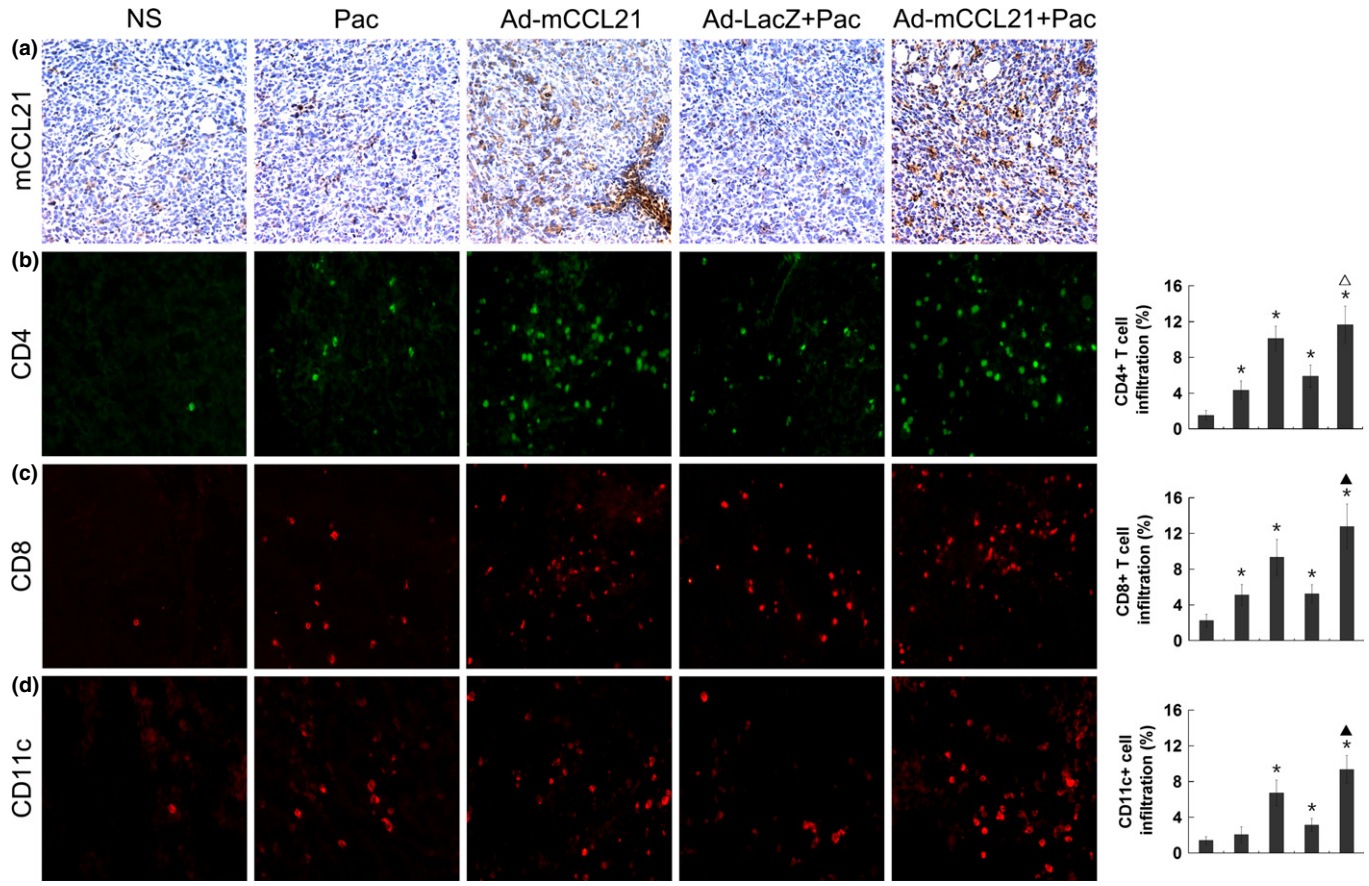

Fig. 5. Expression of at the tumor site attracts the infiltration of immune cells. (a) mCCL21 immunohistochemical peroxidase staining was done on paraffin-embedded tumor sections obtained from each of the five therapy groups: normal saline (NS), paclitaxel (Pac), Ad-mCCL21, Ad-LacZ+-Pac, or Ad-mCCL21+Pac. Significant expression of mCCL21 could be detected in both Ad-mCCL21 and Ad-mCCL21+Pac groups. Representative images of immunofluorescence stained with anti-CD4 (b), anti-CD8 (c), and anti-CD11c (d) antibodies. Significant infiltration of CD4-, CD8-, and CD11c-positive cells in the tumor tissues indicate that Ad-mCCL21 or Ad-mCCL21+Pac treatment would lead to the recruitment and maturation of immune cells. The infiltration of different immune cell subsets was microscopically counted at five randomly chosen high-power fields (×200). The columns in all graphs correspond to the labeled columns in the picture. Bars, ±SD. *$P < 0.01$ relative to NS control. ▲$P < 0.01$ relative to Pac, Ad-mCCL21, or Ad-LacZ+Pac group. △$P < 0.01$ relative to Pac or Ad-LacZ+Pac group.

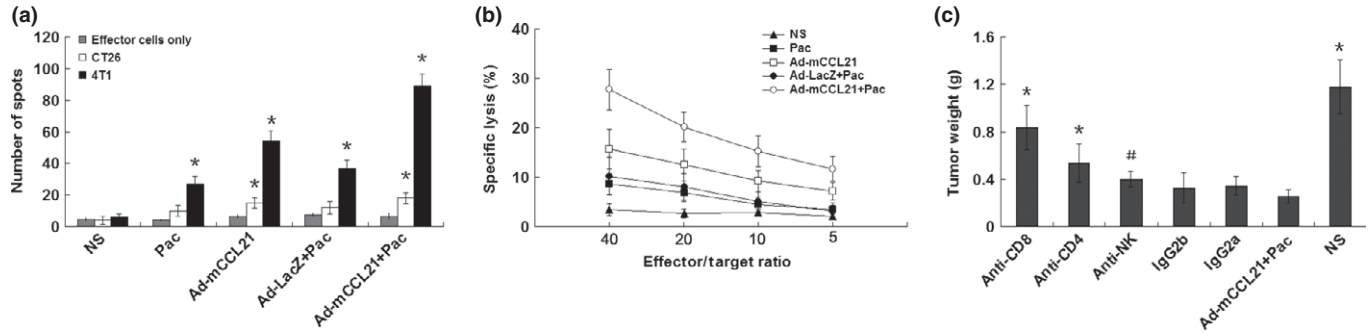

Fig. 6. Specific antitumor responses were enhanced following treatment with Ad-mCCL21 + low-dose paclitaxel (Ad-mCCL21+Pac) therapy. (a) Enzyme-linked immunospot assay. Mouse γ-interferon-specific assay was done, and spots were quantified with an Immunospot Image Analyzer. Compared with treatment with normal saline (NS), paclitaxel (Pac), Ad-mCCL21, or Ad-LacZ+Pac, T lymphocytes from the Ad-mCCL21+Pac-treated group had significantly greater frequency of specific T cells releasing γ-interferon when restimulated with 4T1 cells. There were minimal responses to the control CT26 cells. Bars, ±SD. *$P < 0.01$ relative to NS control. (b) CTL-mediated cytotoxicity *in vitro*. The cytotoxic activity of splenic lymphocytes was measured in 4-h ^{51}Cr-release assay. The purified T lymphocytes were added to ^{51}Cr-labeled 4T1 cells immediately after isolation from spleens. T cells derived from the Ad-mCCL21+Pac-treated mice showed higher cytotoxicity against 4T1 cells than those from the Ad-mCCL21 ($P < 0.05$), Ad-LacZ+Pac ($P < 0.01$), Pac ($P < 0.01$), or NS group ($P < 0.01$). (c) Abrogation of CTL-mediated cytotoxicity *in vivo*. Depletion of $CD4^+$ or $CD8^+$ T lymphocytes or natural killer cells by corresponding mAbs. Depletion of $CD4^+$ or $CD8^+$ T lymphocytes significantly impaired the antitumor activity of Ad-mCCL21+Pac therapy, the depletion of natural killer cells showed partly abrogation. Bars, ±SD. *$P < 0.01$ relative to Ad-mCCL21+Pac therapy. #$P < 0.05$ relative to Ad-mCCL21+Pac therapy.

as weight loss, ruffling of fur, behavior, feeding, or toxic death. No pathologic changes in liver, heart, lung, kidney, spleen, brain, or bone marrow were found by microscopic examination (data not shown). Our results suggested that low-dose paclitaxel in combination with Ad-mCCL21 was concurrently practicable with less host toxicity.

Discussion

In these studies we tested the hypothesis that the combination of low-dose paclitaxel with recombinant adenovirus expressing mCCL21 would improve therapeutic antitumor efficacy. This proved to be the case, as we found that the combined therapy limits the growth and progression of murine cancer more effectively, thereby improving tumor-related cachexia and prolonging survival. Our results indicate that the effects of the combination therapy are associated with increased infiltration of immune cells, altered the immunosuppressive microenvironment, improved tumor cell apoptosis, and reduced new vessel formation in the tumor tissues. We further show that the antitumor activity of the combined treatment could be partly abrogated by the depletion of $CD4^+$ or $CD8^+$ T lymphocytes, which suggested these antitumor immune responses are dependent on both $CD4^+$ helper and $CD8^+$ cytotoxic T cells. Importantly, the enhancement of antitumor activity occurred without an ensuing increase in host toxicity or signs of acquired drug resistance during the course of treatment.

Tumor cells, together with tumor-infiltrating stromal cells, produce a variety of growth factors and cytokines with autocrine and paracrine functions, which enables them to progress to a more aggressive phenotype and escape the surveillance of the immune system.[22] Thus, altered cytokine networks in the tumor microenvironment may contribute to the dysregulation of cellular functions in cancer cells. It has been shown that significant change in cytokine profiles can be observed in tumor sites after intratumoral delivery of CCL21.[13–17] Our findings that the cytokine production from tumor tissues (GM-CSF, IFN-γ, MIG, IP-10, IL-12, TGF-β, IL-10, and VEGF) was significantly altered by Ad-mCCL21 or Ad-mCCL21+Pac therapy are in agreement with previous reports. Moreover, the combined treatment synergistically reduced the immunosuppressive molecule IL-10 and angiogenesis factor VEGF, and increased GM-CSF, IFN-γ, MIG, IP-10, and IL-12 within the tumor sites. Thus, the combined therapy may benefit from the synergistic altering cytokines by improving antigen presentation, CTL generation, and angiogenesis limitation.

In the tumor microenvironment, VEGF can be produced by various cell types, including tumor cells, inflammatory and stromal cells, platelets and vascular cells.[29] Overexpressing TGF-β can be observed in many cancer cells (including B16-F10 and 4T1), and the elevation of TGF-β is correlated with tumor progression, invasion, metastases, and poor prognosis.[30,31] It has been reported that the full potency of CCL21-mediated antitumor response required the induction of IFN-γ, MIG, and IP10 in concert,[32] which is in agreement with our findings (Fig. 4a). Both MIG and IP10 are potent inhibitors of angiogenesis that can limit new vessel growth by binding to CXCR3 on endothelial cells and triggering endothelial cell anoikis, thus downregulating the expression of VEGF by endothelial cells.[33,34] Moreover, reducing microvessel density would lead to the observed increase in both tumor cell apoptosis and necrosis, and block the tumor cells to express VEGF and TGF-β. Transforming growth factor-β is one of the immune inhibitory cytokines that may potently suppress Ag presentation and antagonize CTL generation and macrophage activities, thus enabling the tumor to escape immune detection.[13] The decrease in TGF-β at the tumor site after CCL21 treatment may have contributed to an increase in antitumor immunity. Thus, we may speculate that the decreasing expression of TGF-β at the tumor site is not only a result but also a reason of the decrease of tumor volume. Further studies will be necessary to delineate the exact mechanism by which CCL21 suppresses the expression of cytokines.

Angiogenesis, a key regulatory factor in tumor growth and metastasis, is tightly regulated by many positive and negative factors, and antiangiogenic therapy has become a potential antitumor strategy.[25,35–37] Here we showed that combined treatment with Ad-mCCL21 and paclitaxel led to enhanced antiangiogenic effectiveness as compared with either treatment alone. The effectiveness of this approach is likely attributable to the cascade of events that are initiated within the tumor microenvironment by delivery of Ad-mCCL21 and low-dose paclitaxel. At the outset, although CCL21 has been identified as a ligand for CCR7, recent studies have shown that mCCL21 can signal through mCXCR3 and share some of the activities of MIG and IP10, including their antiangiogenic activity.[15,38,39] In this regard, Ad-mCCL21 treatment may directly inhibit the formation of neoangiogenesis in the tumor bed. In addition, a significant increase in the expression of angiostatic factors MIG and IP10 can be observed in the tumor tissues of the Ad-mCCL21+Pac-treated group. Hence, the antiangiogenic activities of the combined therapy may in part due to the increase in antiangiogenic proteins MIG and IP10. Furthermore, growing evidence suggests that frequent administration of low doses of chemotherapeutic agents could inhibit angiogenesis by targeting tumor-associated endothelial cells.[40–44] Thus, the combined therapy could maximize the growth-limiting effects on the tumor vasculature. The enhanced antiangiogenic activities of the combined therapy would lead to observed increase in both tumor cell apoptosis and necrosis. This may, in turn, improve the presentation of tumor antigens from the dying tumor cells to T lymphocytes and thus support antitumor immunity.

The breaking of immune tolerance against tumor-associated antigens and induction of autoimmunity against tumors should be a useful approach for the treatment of tumors.[45–47] Although it is common to consider conventional cytotoxic chemotherapy as an immunosuppressive modality, more recent studies have indicated that some cytotoxic drugs have the ability to disrupt pathways of immune suppression and immune tolerance in a manner that depends on the drug type, its dose, and the treatment schedule in relation to the immune-based intervention.[48] Clinical evidence also suggests that standard dose chemotherapy can affect the human immune system in both negative and positive ways.[49] In this context, the treatment time of standard dose chemotherapy drugs should be carefully dissected for integrating with immune-based therapies, to achieve the greatest long-term clinical benefit for cancer patients. Alternatively, low dose chemotherapy may more efficiently augment antitumor immunity by a variety of mechanisms.[50,51] It has been shown that chemotherapeutic agents in non-cytotoxic concentrations are capable of triggering the release of danger signals from dying tumor cells, increasing the immunogenicity of tumor cells, upregulating the ability of DCs to present Ags to Ag-specific T cells, and altering the immune tolerance of the tumor environment.[22,23,48,52,53] The data in the present study showed that combined treatment with Ad-mCCL21 and paclitaxel led to enhanced antitumor growth

and the increased infiltration of $CD4^+$, $CD8^+$, and $CD11c^+$ cells in the tumor tissues compared with the Pac, Ad-mCCL21, Ad-LacZ+Pac, or no-treatment groups. In addition, the depletion of $CD8^+$ or $CD4^+$ lymphocytes showed partial abrogation of the antitumor activity of the combination therapy *in vivo*, which indicates the antitumor immunity of the combination therapy is dependent on both $CD4^+$ helper and $CD8^+$ cytotoxic T cells.

In conclusion, we showed that the combination of CCL21 with low-dose paclitaxel significantly enhanced the antitumor activity compared with either treatment alone. These enhanced antitumor efficacies functioned by altering the intratumoral microenvironment, limiting tumor angiogenesis, inducing tumor cell apoptosis, and infiltration of lymphocytes. The present findings may prove useful in further explorations of the potential application of this combined approach in the treatment of malignant cancer.

Acknowledgments

This work was supported by The National Key Basic Research Program (973 Program) of China (Grant nos 2010CB529900 and 2010CB529906), and the Hi-tech Research and Development Program (863 Program) of China (Grant nos 2007AA021106 and 2006AA02Z488).

Disclosure Statement

The authors have no conflict of interest.

References

1 Huang AY, Golumbek P, Ahmadzadeh M, Jaffee E, Pardoll D, Levitsky H. Role of bone marrow-derived cells in presenting MHC class I-restricted tumor antigens. *Science* 1994; **264**: 961–5.
2 Smyth MJ, Crowe NY, Hayakawa Y, Takeda K, Yagita H, Godfrey DI. NKT cells-conductors of tumor immunity? *Curr Opin Immunol* 2002; **14**: 165–71.
3 van Mierlo GJ, Boonman ZF, Dumortier HM *et al.* Activation of dendritic cells that cross-present tumor-derived antigen licenses $CD8^+$ CTL to cause tumor eradication. *J Immunol* 2004; **173**: 6753–9.
4 Restifo NP, Esquivel F, Kawakami Y *et al.* Identification of human cancers deficient in antigen processing. *J Exp Med* 1993; **177**: 265–72.
5 Frey AB, Monu N. Signaling defects in anti-tumor T cells. *Immunol Rev* 2008; **222**: 192–205.
6 Bonecchi R, Locati M, Mantovani A. Chemokines and cancer: a fatal attraction. *Cancer Cell* 2011; **19**: 434–5.
7 Lira SA, Furtado GC. The biology of chemokines and their receptors. *Immunol Res* 2012; **54**: 111–20.
8 Gunn MD, Tangemann K, Tam C, Cyster JG, Rosen SD, Williams LT. A chemokine expressed in lymphoid high endothelial venules promotes the adhesion and chemotaxis of naive T lymphocytes. *Proc Natl Acad Sci USA* 1998; **95**: 258–63.
9 Willimann K, Legler DF, Loetscher M *et al.* The chemokine SLC is expressed in T cell areas of lymph nodes and mucosal lymphoid tissues and attracts activated T cells via CCR7. *Eur J Immunol* 1998; **28**: 2025–34.
10 Riedl K, Baratelli F, Batra RK *et al.* Overexpression of CCL-21/secondary lymphoid tissue chemokine in human dendritic cells augments chemotactic activities for lymphocytes and antigen presenting cells. *Mol Cancer* 2003; **2**: 35.
11 Cyster JG. Chemokines and the homing of dendritic cells to the T cell areas of lymphoid organs. *J Exp Med* 1999; **189**: 447–50.
12 Chan VW, Kothakota S, Rohan MC *et al.* Secondary lymphoid-tissue chemokine (SLC) is chemotactic for mature dendritic cells. *Blood* 1999; **93**: 3610–6.
13 Sharma S, Stolina M, Luo J *et al.* Secondary lymphoid tissue chemokine mediates T cell-dependent antitumor responses *in vivo*. *J Immunol* 2000; **164**: 4558–63.
14 Yang SC, Batra RK, Hillinger S *et al.* Intrapulmonary administration of CCL21 gene-modified dendritic cells reduces tumor burden in spontaneous murine bronchoalveolar cell carcinoma. *Cancer Res* 2006; **66**: 3205–13.
15 Liang CM, Zhong CP, Sun RX *et al.* Local expression of secondary lymphoid tissue chemokine delivered by adeno- associated virus within the tumor bed stimulates strong anti-liver tumor immunity. *J Virol* 2007; **81**: 9502–11.
16 Kar UK, Srivastava MK, Andersson A *et al.* Novel CCL21-vault nanocapsule intratumoral delivery inhibits lung cancer growth. *PLoS ONE* 2011; **6**: e18758.
17 Chen L, Zhou S, Qin J *et al.* Combination of SLC administration and Tregs depletion is an attractive strategy for targeting hepatocellular carcinoma. *Mol Cancer* 2013; **12**: 153.
18 Spencer CM, Faulds D. Paclitaxel. A review of its pharmacodynamic and pharmacokinetic properties and therapeutic potential in the treatment of cancer. *Drugs* 1994; **48**: 794–847.
19 Weng D, Song X, Xing H *et al.* Implication of the Akt2/survivin pathway as a critical target in paclitaxel treatment in human ovarian cancer cells. *Cancer Lett* 2009; **273**: 257–65.
20 Shaked Y, Emmenegger U, Francia G *et al.* Low-dose metronomic combined with intermittent bolus-dose cyclophosphamide is an effective long-term chemotherapy treatment strategy. *Cancer Res* 2005; **65**: 7045–51.
21 Shaked Y, Emmenegger U, Man S *et al.* Optimal biologic dose of metronomic chemotherapy regimens is associated with maximum antiangiogenic activity. *Blood* 2005; **106**: 3058–61.
22 Zhong H, Han B, Tourkova IL *et al.* Low-dose paclitaxel prior to intratumoral dendritic cell vaccine modulates intratumoral cytokine network and lung cancer growth. *Clin Cancer Res* 2007; **13**: 5455–62.
23 He Q, Li J, Yin W *et al.* Low-dose paclitaxel enhances the anti-tumor efficacy of GM-CSF surface-modified whole-tumor-cell vaccine in mouse model of prostate cancer. *Cancer Immunol Immunother* 2011; **60**: 715–30.
24 Yang L, Wang L, Su XQ *et al.* Suppression of ovarian cancer growth via systemic administration with liposome-encapsulated adenovirus-encoding endostatin. *Cancer Gene Ther* 2010; **17**: 49–57.
25 Li G, Tian L, Hou JM *et al.* Improved therapeutic effectiveness by combining recombinant CXC chemokine ligand 10 with Cisplatin in solid tumors. *Clin Cancer Res* 2005; **11**: 4217–24.
26 Wang YS, Li D, Shi HS *et al.* Intratumoral expression of mature human neutrophil peptide-1 mediates antitumor immunity in mice. *Clin Cancer Res* 2009; **15**: 6901–11.
27 Mandic M, Almunia C, Vicel S *et al.* The alternative open reading frame of LAGE-1 gives rise to multiple promiscuous HLA-DR-restricted epitopes recognized by T-helper 1-type tumor-reactive $CD4^+$ T cells. *Cancer Res* 2003; **63**: 6506–15.
28 Wei YQ, Wang QR, Zhao X *et al.* Immunotherapy of tumors with xenogeneic endothelial cells as a vaccine. *Nat Med* 2000; **6**: 1160–6.
29 Greenberg JI, Cheresh DA. VEGF as an inhibitor of tumor vessel maturation: implications for cancer therapy. *Expert Opin Biol Ther* 2009; **9**: 1347–56.
30 Liu B, Zhang H, Li J *et al.* Triptolide downregulates Treg cells and the level of IL-10, TGF-β, and VEGF in melanoma-bearing mice. *Planta Med* 2013; **79**: 1401–7.
31 Taylor MA, Davuluri G, Parvani JG *et al.* Upregulated WAVE3 expression is essential for TGF-β-mediated EMT and metastasis of triple-negative breast cancer cells. *Breast Cancer Res Treat* 2013; **142**: 341–53.
32 Sharma S, Yang SC, Hillinger S *et al.* SLC/CCL21-mediated anti-tumor responses require IFNgamma, MIG/CXCL9 and IP-10/CXCL10. *Mol Cancer* 2003; **2**: 22.
33 Bodnar RJ, Yates CC, Rodgers ME, Du X, Wells A. IP-10 induces dissociation of newly formed blood vessels. *J Cell Sci* 2009; **122**: 2064–77.
34 Keeley EC, Mehrad B, Strieter RM. CXC chemokines in cancer angiogenesis and metastases. *Adv Cancer Res* 2010; **106**: 91–111.
35 Folkman J. Seminars in Medicine of the Beth Israel Hospital, Boston. Clinical applications of research onangiogenesis. *N Engl J Med* 1995; **333**: 1757–63.
36 Marx J. Angiogenesis. A boost for tumor starvation. *Science* 2003; **301**: 452–4.
37 Albini A, Tosetti F, Li VW, Noonan DM, Li WW. Cancer prevention by targeting angiogenesis. *Nat Rev Clin Oncol* 2012; **9**: 498–509.
38 Soto H, Wang W, Strieter RM *et al.* The CC chemokine 6Ckine binds the CXC chemokine receptor CXCR3. *Proc Natl Acad Sci USA* 1998; **95**: 8205–10.
39 Chun L, Yin CC, Song JZ *et al.* Soluble expression of recombinant human secondary lymphoid chemokine (SLC) in E. coli and research on its *in vitro* and *in vivo* bioactivity. *J Biochem* 2004; **136**: 769–76.
40 Kamat AA, Kim TJ, Landen CN Jr *et al.* Metronomic chemotherapy enhances the efficacy of antivascular therapy in ovarian cancer. *Cancer Res* 2007; **67**: 281–8.

41 Chen CA, Ho CM, Chang MC *et al.* Metronomic chemotherapy enhances antitumor effects of cancer vaccine by depleting regulatory T lymphocytes and inhibiting tumor angiogenesis. *Mol Ther* 2010; **18**: 1233–43.
42 Naganuma Y, Choijamts B, Shirota K *et al.* Metronomic doxifluridine chemotherapy combined with the anti-angiogenic agent TNP-470 inhibits the growth of human uterine carcinosarcoma xenografts. *Cancer Sci* 2011; **102**: 1545–52.
43 Torimura T, Iwamoto H, Nakamura T *et al.* Metronomic chemotherapy: possible clinical application in advanced hepatocellular carcinoma. *Transl Oncol* 2013; **6**: 511–9.
44 Lien K, Georgsdottir S, Sivanathan L, Chan K, Emmenegger U. Low-dose metronomic chemotherapy: a systematic literature analysis. *Eur J Cancer* 2013; **49**: 3387–95.
45 Luo Y, Wen YJ, Ding ZY *et al.* Immunotherapy of tumors with protein vaccine based on chicken homologous Tie-2. *Clin Cancer Res* 2006; **12**: 1813–9.
46 Bae J, Smith R, Daley J *et al.* Myeloma-specific multiple peptides able to generate cytotoxic T lymphocytes: a potential therapeutic application in multiple myeloma and other plasma cell disorders. *Clin Cancer Res* 2012; **18**: 4850–60.
47 Higashihara Y, Kato J, Nagahara A *et al.* Phase I clinical trial of peptide vaccination with URLC10 and VEGFR1 epitope peptides in patients with advanced gastric cancer. *Int J Oncol* 2014; **44**: 662–8.
48 Chen G, Emens LA. Chemoimmunotherapy: reengineering tumor immunity. *Cancer Immunol Immunother* 2013; **62**: 203–16.
49 Emens LA. Chemoimmunotherapy. *Cancer J* 2010; **16**: 295–303.
50 Weir GM, Liwski RS, Mansour M. Immune modulation by chemotherapy or immunotherapy to enhance cancer vaccines. *Cancers (Basel)* 2011; **3**: 3114–42.
51 Koumarianou A, Christodoulou MI, Patapis P *et al.* The effect of metronomic versus standard chemotherapy on the regulatory to effector T-cell equilibrium in cancer patients. *Exp Hematol Oncol* 2014; **3**: 3.
52 Shurin GV, Tourkova IL, Kaneno R, Shurin MR. Chemotherapeutic agents in noncytotoxic concentrations increase antigen presentation by dendritic cells via an IL-12-dependent mechanism. *J Immunol* 2009; **183**: 137–44.
53 Fridlender ZG, Sun J, Singhal S *et al.* Chemotherapy delivered after viral immunogene therapy augments antitumor efficacy via multiple immune-mediathhed mechanisms. *Mol Ther* 2010; **18**: 1947–59.